

Simultaneous dispersion measurements of multiple fiber modes using virtual reference interferometry

Michael A. Galle,^{1,*} Simarjeet S. Saini,² Waleed S. Mohammed,³ Pierre Sillard,⁴ and Li Qian¹

¹Dept. of Elec. and Comp. Engineering, Univ. of Toronto, 10 King's College Road, Toronto, On., Canada

²Dept. of Elec. and Comp. Engineering, Univ. of Waterloo, 200, University Avenue W., Waterloo, On., Canada

³Center of Optoelectronics, Communication and Control Systems (BU-CROCCS), School of Engineering, Bangkok University, Pahunyouthin Road, Phatumthani, 12120, Thailand

⁴Prismian Group, Parc des Industries Artois Flandres, 644 boul. Est, Billy Berclau, 62092 Haisnes Cedex, France
*michael.galle@utoronto.ca

Abstract: We present the simultaneous measurement of first and second order dispersion in short length (<1m) few mode fibers (polarization and transverse) using virtual reference interferometry. This technique generates results equivalent to balanced spectral interferometry, without the complexity associated with physical balancing. This is achieved by simulating a *virtual reference* with a group delay equal to that of the physical interferometer. The amplitude modulation that results from mixing the interferograms, generated in both the unbalanced interferometer and the virtual reference, is equivalent to the first order interference that would be produced by physical balancing. The advantages of the technique include speed, simplicity, convenience and the capability for simultaneous measurement of multiple modes. The theoretical framework is first developed and then verified experimentally.

© 2014 Optical Society of America

OCIS codes: (060.2270) Fiber characterization; (060.2420) Fibers, polarization-maintaining; (120.3180) Interferometry; (120.3930) Metrological instrumentation.

References and links

1. F. Yaman, N. Bai, B. Zhu, T. Wang, and G. Li, "Long distance transmission in few-mode fibers," *Opt. Express* **18**(12), 13250–13257 (2010).
2. P. Sillard, M. Astruc, D. Boivin, H. Maerten, and L. Provost, "Few-Mode Fiber for Uncoupled Mode-Division Multiplexing Transmissions," in 37th European Conference and Exposition on Optical Communications, OSA Technical Digest (CD) (Optical Society of America, 2011), paper Tu.5.LeCervin.7.
3. S. Randel, R. Ryf, A. Sierra, P. J. Winzer, A. H. Gnauck, C. A. Bolle, R. J. Essiambre, D. W. Peckham, A. McCurdy, and R. Lingle, Jr., "6×56-Gb/s mode-division multiplexed transmission over 33-km few-mode fiber enabled by 6×6 MIMO equalization," *Opt. Express* **19**(17), 16697–16707 (2011).
4. C. Koebele, M. Salsi, D. Sperti, P. Tran, P. Brindel, H. Mardoyan, S. Bigo, A. Boutin, F. Verluise, P. Sillard, M. Astruc, L. Provost, F. Cerou, and G. Charlet, "Two mode transmission at 2×100 Gb/s, over 40 km-long prototype few-mode fiber, using LCOS-based programmable mode multiplexer and demultiplexer," *Opt. Express* **19**(17), 16593–16600 (2011).
5. F. Yaman, N. Bai, Y. K. Huang, M. F. Huang, B. Zhu, T. Wang, and G. Li, "10 x 112Gb/s PDM-QPSK transmission over 5032 km in few-mode fibers," *Opt. Express* **18**(20), 21342–21349 (2010).
6. A. Galtarossa, L. Palmieri, M. Schiano, and T. Tambosso, "Single-End Polarization Mode Dispersion Measurement Using Backreflected Spectra Through a Linear Polarizer," *J. Lightw. Tech.* **17**(10), 1835–1842 (1999).
7. B. L. Heffner, "Automated Measurement of Polarization Mode Dispersion Using Jones Matrix Eigenanalysis," *IEEE Photon. Technol. Lett.* **4**(9), 1066–1069 (1992).
8. B. L. Heffner, "Accurate, Automated Measurement of Differential Group Delay Dispersion and Principle State Variation Using Jones Matrix Eigenanalysis," *IEEE Photon. Technol. Lett.* **5**(7), 814–817 (1993).
9. F. Tang, X. Z. Wang, Y. Zhang, and W. Jing, "Distributed measurement of birefringence dispersion in polarization-maintaining fibers," *Opt. Lett.* **31**(23), 3411–3413 (2006).

10. F. Tang, X. Z. Wang, Y. Zhang, and W. Jing, "Characterization of birefringence dispersion in polarization-maintaining fibers by use of white-light interferometry," *Appl. Opt.* **46**(19), 4073–4080 (2007).
11. D. A. Flavin, R. McBride, and J. D. Jones, "Dispersion of birefringence and differential group delay in polarization-maintaining fiber," *Opt. Lett.* **27**(12), 1010–1012 (2002).
12. M. G. Shlyagin, A. V. Khomenko, and D. Tentori, "Birefringence dispersion measurement in optical fibers by wavelength scanning," *Opt. Lett.* **20**(8), 869–871 (1995).
13. R. Posey, L. Phillips, D. Diggs, and A. Sharma, "LP01-LP02 interference using a spectrally extended light source: measurement of the non-step-refractive-index profile of optical fibers," *Opt. Lett.* **21**(17), 1357–1359 (1996).
14. P. Hlubina, "Measuring intermodal dispersion in optical fibres using white-light spectral interferometry with the compensated Michelson interferometer," *J. Mod. Opt.* **48**(14), 2087–2096 (2001).
15. P. Hlubina, T. Martynkien, and W. Urbanczyk, "Measurements of intermodal dispersion in few-mode optical fibres using a spectral-domain white-light interferometric method," *Meas. Sci. Technol.* **14**(6), 784–789 (2003).
16. J. W. Nicholson, A. D. Yablon, S. Ramachandran, and S. Ghalmi, "Spatially and spectrally resolved imaging of modal content in large-mode-area fibers," *Opt. Express* **16**(10), 7233–7243 (2008).
17. K. Jespersen, Z. Li, L. Gruner-Nielsen, B. Palsdottir, F. Poletti, and J. W. Nicholson, "Measuring Distributed Mode Scattering in Long, Few-Moded Fibers," in *Optical Fiber Communication Conference, OSA Technical Digest (Optical Society of America, 2012)*, paper OTh31.4.
18. J. Cheng, M. E. V. Pedersen, K. Wang, C. Xu, L. Gruner-Nielsen, and D. Jakobsen, "Time-domain multimode dispersion measurement in a higher-order-mode fiber," *Opt. Lett.* **37**(3), 347–349 (2012).
19. Y. Z. Ma, Y. Sych, G. Onishchukov, S. Ramachandran, U. Peschel, B. Schmauss, and G. Leuchs, "Fiber-modes and fiber-anisotropy characterization using low-coherence interferometry," *Appl. Phys. B* **96**(2-3), 345–353 (2009).
20. W. Mohammed, J. Meier, M. A. Galle, L. Qian, J. S. Aitchison, and P. W. E. Smith, "Linear and quadratic dispersion characterization of millimeter-length fibers and waveguides using common-path interferometry," *Opt. Lett.* **32**(22), 3312–3314 (2007).
21. M. Takeda, H. Ina, and S. Kobayashi, "Fourier-transform method of fringe-pattern analysis for computer-based topography and interferometry," *J. Opt. Soc. Am.* **72**(1), 156–160 (1982).
22. P. Merrit, R. P. Tatum, and D. A. Jackson, "Interferometric chromatic dispersion measurements on short lengths of monomode optical fiber," *J. Lightwave Technol.* **7**(4), 703–716 (1989).
23. P. Hlubina, D. Ciprian, M. Kadulova, T. Martynkien, P. Mergo, and W. Urbanczyk, "Spectral interferometry-based dispersion characterization of microstructured and specialty optical fibers using a supercontinuum source," *Proc. SPIE* **8426**, 84260N (2012).
24. M. A. Galle, S. S. Saini, W. S. Mohammed, and L. Qian, "Chromatic dispersion measurements using a virtually referenced interferometer," *Opt. Lett.* **37**(10), 1598–1600 (2012).
25. M. A. Galle, S. S. Saini, W. S. Mohammed, and L. Qian, "Virtual reference interferometry: theory and experiment," *J. Opt. Soc. Am. B* **29**(11), 3201–3210 (2012).

1. Introduction

Few-mode fibers (FMFs) have attracted considerable research interest [1–5] due to their compatibility with currently deployed single mode fibers and their resistance to intermodal coupling [1]. This has made them excellent candidates for space-division multiplexing (SDM) systems that can be used for increasing network capacity. Recently, high-capacity transmission systems that use a combination of transverse and polarization mode multiplexed signals have been demonstrated [3, 4]. The design of these systems requires accurate dispersion characterization of both types of modes.

Early characterization techniques focused almost exclusively on measuring the differential group delay (DGD) between two polarization modes, such as those present in a polarization maintaining (PM) fiber. Several techniques were developed for this purpose including those based on: Polarizer-analyser [6], Jones matrix eigenanalysis [7, 8], temporal interferometry [9–11] and spectral interferometry [12–14]. These DGD-based techniques measure the interference pattern produced when the phase front in one mode interferes with that in another. These techniques work very well for the characterization of a fiber with two modes; however, potentially ambiguous results can be produced as the number of modes increases [15–17]. The problem occurs when the power in a higher-order mode is comparable to that of the fundamental [16] as it becomes difficult to determine if a beat frequency in the interference pattern is caused by interference between the fundamental and a higher-order mode or the interference between two higher-order modes. Time-of-flight (TOF) and interferometric techniques, capable of measuring the *absolute* group delay of a given mode

are immune to this type of ambiguity. A recent TOF demonstration characterized the dispersion of FMF [18] using a high speed (30GHz) sampling oscilloscope and pulsed-tunable laser to characterize. This measurement, however, required a 10.2 meter length FMF. For the characterization of shorter fiber lengths (<1 meter), however, TOF techniques place prohibitive requirements on the sampling oscilloscope and pulsed laser. Interferometric techniques, on the other hand, are well suited for short length characterization. Temporal interferometric techniques (white-light interferometry) are capable of measuring the absolute group delay of each mode in an FMF [19]; however, they are susceptible to the vibrational noise caused by a moving variable delay line. Spectral interferometric techniques, on the other hand, utilize a stationary reference arm and are generally preferred because they are not susceptible to this kind of vibrational noise. Some spectral interferometric based techniques employ a Fast Fourier Transform (FFT) to measure group delay from an unbalanced interferometer [20, 21]. The difficulty with using this approach for measuring the dispersion in an FMF is that the spatial frequency peak generated by the FFT depends on the size of the spectral window used in the FFT. A window that is too large produces a broadened peak due to dispersion and a window that is too narrow generates a broadened peak due to the inverse nature of the bandwidth between a signal and its FFT. Since there is no way to know a priori the optimum window size for the FFT, in short length fibers it is difficult to prevent the overlap between spatial frequency peaks and isolate individual modes. An additional limitation of FFT based techniques is that the second order dispersion can only be obtained from a fit to the measured group delay curve (not directly from the interferogram). This can be a problem for fibers with several modes where the coupled power in each mode is low, resulting in a low signal-to-noise ratio (SNR) and higher noise in the group delay curve.

Techniques based on balanced spectral interferometry (BSI) [22, 23] do not suffer from the issues associated with using a spectral window since they use the entire scan bandwidth. Additionally they are capable of extracting the second order dispersion directly from the interferogram, independent of the group delay measurement. BSI techniques have been demonstrated in the measurement of group delay in polarization modes of birefringent fiber [23], however, to the best of the authors' knowledge this capability has not been demonstrated for transverse modes in an FMF with more than two modes. The drawback of using BSI based techniques, however, is that they require a *physical* reference for balancing. This involves the need for calibration and makes them susceptible to environmental fluctuations (requiring the enclosure and isolation of the reference path). An important consideration when using BSI for dispersion measurements is that the construction and use of a free-space variable delay line is not trivial. In addition, since each point in the dispersion curve requires a separate interference scan, BSI measurements suffer from long experiment run times.

Virtual reference interferometry (VRI), proposed by us in [24, 25], is useful for overcoming these issues since it has all the functionality and advantages of BSI but removes the need for a physical reference. In VRI, a physically generated spectral interferogram (produced using an unbalanced interferometer such as a Fabry-Perot interferometer) is mixed via point-wise multiplication with a simulated spectral interferogram (typically produced by a simulating a free-space interferometer with a group delay equal to the imbalance in the interferometer at a given wavelength). The low frequency amplitude modulation in the resulting second order interference pattern is equivalent to the first order interference that would be produced by physical balancing in BSI. VRI has recently been demonstrated for the measurement of dispersion in single mode fibers and devices [24, 25]. The focus of this manuscript is to demonstrate the advantages of its application in the measurement of first and second order dispersion of each mode (polarization and transverse) in an FMF. We also highlight that, for modes with sufficient spatial separation, plots of first and second order dispersion can be generated simultaneously, without the possibility for ambiguity in the results.

2. Theory

Polarization modes

Dispersion measurements that employ VRI typically use the interference generated by the reflections at the front and end facets of a fiber under test (Fabry-Perot configuration) to take advantage of the simplicity of single-ended measurements. For a PM fiber (modeled in Fig. 1) the reflected electric fields are $\bar{U}_o = A_1\hat{i} + A_2\hat{j}$ and $U_1 = A_1e^{-2j\beta_1L_f}\hat{i} + A_2e^{-2j\beta_2L_f}\hat{j}$, where β_1 and β_2 are the propagation constant in the fast and slow axis as a function of wavelength λ and L_f is the fiber length. A_1 and A_2 are the field amplitudes of the fast and slow components respectively, which remain constant for \bar{U}_o and \bar{U}_1 assuming there is no mode coupling.

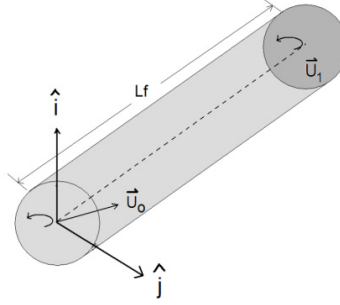


Fig. 1. Model for the interference in a polarization maintaining fiber.

The interference pattern generated by the reflected electric fields are described by Eq. (1a)

$$I_{Real}(\lambda) = |\bar{U}_o + \bar{U}_1|^2 \quad (1a)$$

$$= 4K + 2(K + \Delta)\cos(2\beta_1L_f) + 2(K - \Delta)\cos(2\beta_2L_f)$$

Where $K = (A_1^2 + A_2^2)/2$ and $\Delta = (A_1^2 - A_2^2)/2$. If we set $\Delta = 0$ by exciting the fiber with an input polarization 45° from fast axis, and remove the DC term, then Eq. (1a) simplifies to Eq. (1b)

$$I_{Real}(\lambda)' = 4K \left(\underbrace{\cos(L_f(\beta_1 - \beta_2))\cos(L_f(\beta_1 + \beta_2))}_{\text{Low freq. (Diff)}} \right) \quad (1b)$$

Setting $\Delta = 0$ is not necessary for the measurements but it simplifies the mathematical expression. Using VRI the first and second order dispersion are extracted via point-by-point multiplication of the real interference pattern, described by Eq. (1b), with a suitable virtual reference interferogram [24, 25] described by Eq. (2)

$$I_{virtual}(\lambda, \hat{\lambda}) = \cos(2k_0L_v(\hat{\lambda}_w)) \quad (2)$$

where k_0 is the free-space propagation constant, L_v is the length of the simulated virtual reference path and $\hat{\lambda}_w$ is the ‘balanced wavelength’ of mode w at which the group delay of the virtual reference path equals that of the measured mode as illustrated in Fig. 2. After filtering out the DC term, the result simplifies to a second-order interference pattern described by Eq. (3):

$$I_{SO}(\lambda, \hat{\lambda}_w) = K \left(\underbrace{\cos(2(\beta_1 L_f - k_0 L_v(\hat{\lambda}_w)))}_{\text{Lowest freq. (Fast axis)}} + \underbrace{\cos(2(\beta_2 L_f - k_0 L_v(\hat{\lambda}_w)))}_{\text{Lowest freq. (Slow axis)}} \right) + \underbrace{2 \cos(L_f(\beta_1 - \beta_2))}_{\text{Low freq. (Diff)}} \underbrace{\cos(L_f(\beta_1 + \beta_2) + 2k_0 L_v(\hat{\lambda}_w))}_{\text{Carrier}} \quad (3)$$

Each of the first two terms in Eq. (3) produces a low-frequency amplitude modulation around its corresponding balanced wavelength, given in Fig. 2 by $\hat{\lambda}_1$ for the slow axis and $\hat{\lambda}_2$ for the fast axis. Away from the balanced wavelength, the modulation frequency increases. If $\hat{\lambda}_1$ and $\hat{\lambda}_2$ are sufficiently separated, the influence on the low-frequency amplitude modulation around $\hat{\lambda}_1$ produced by the second term (cross talk), or the influence on $\hat{\lambda}_2$ by the first term, can be easily removed by low-pass filtering. The third term in Eq. (3) can also be low-pass filtered since it contains a slowly varying cosine (envelope) that modulates a fast varying cosine, and therefore has a zero average value. The inset of Fig. 2 (showing a magnified region near $\hat{\lambda}_1$) shows the carrier (not resolved and appearing black) modulated by multiple ‘envelopes’ of different frequencies. The lowest-frequency amplitude modulation is used to locate $\hat{\lambda}_1$ and $\hat{\lambda}_2$, from which the group delay of each mode is obtained. Plots of the first and second order dispersion vs. wavelength can be produced by varying $L_v(\hat{\lambda}_w)$ as described in [24, 25]. This process can then be repeated for other modes by scanning $L_v(\hat{\lambda}_w)$ over different ranges. The precision of identifying balance wavelengths improves by removing sources of noise such as the high frequency carrier and cross talk from adjacent modes. This is achieved by low pass filtering, as shown in the lower plot of Fig. 2. Sustaining low error in the process requires sufficient spectral separation $\hat{\lambda}_2 - \hat{\lambda}_1$. This occurs as long as the wavelength location of the second peak to the left of $\hat{\lambda}_1$ is greater than the wavelength location of the second peak to the right of $\hat{\lambda}_2$. Following the analysis in [25] this condition is satisfied by Eq. (4)

$$\hat{\lambda}_2 - \hat{\lambda}_1 \geq \frac{1}{2} \sum_{w=1}^2 \frac{\sqrt{6}}{(cL_f D(\hat{\lambda}_w))^{1/2}} \hat{\lambda}_w \quad (4)$$

where $D(\hat{\lambda}_w)$ is the second-order dispersion parameter of mode w and c is the speed of light.

Using typical dispersion parameters of SMF28, modes having a group index difference greater than 2.75×10^{-4} for a 1m long fiber can be resolved. We must note, however, that the maximum fiber length that can be characterized, using the common-path configuration, is dependent on the spectral resolution $\Delta\lambda$ with which the interferogram is sampled, and is described by $L_f \leq \lambda^2 / (20N_g \Delta\lambda)$ [25]. The maximum measurable fiber length (typically ~0.8m) is sufficient for many applications, especially those in which only short lengths of fiber are available or desired. Additionally, for few mode fibers it is desired to keep the mode separation described by Eq. (4) large enough to ensure resistance to intermodal coupling. As a result, there is no need to use long lengths of fiber to reduce the minimum spectral separation in Eq. (4) and therefore the fiber length is not a limitation for most practical cases.

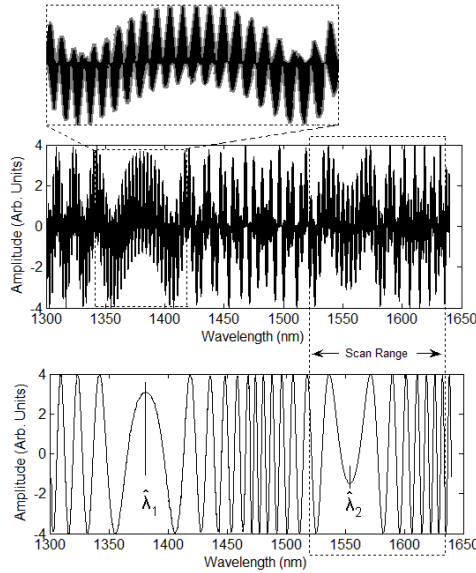


Fig. 2. Simulated second order interference pattern (upper graph) and the result of low-pass filtering (lower graph) used to extract the balance wavelengths, from which absolute group delay and second order dispersion of the individual modes can be obtained. Inset above shows a magnified spectral region around a balance wavelength. Although both modes (the slow axis balanced at $\hat{\lambda}_1$ and the fast axis balanced at $\hat{\lambda}_2$) are illustrated in the figure, only one mode is typically within the scan range of the tunable laser for a given L_f , which is varied to extract group delay and second order dispersion of both modes as a function of wavelength.

Transverse Modes

A model for the reflections at the facets of a p-moded FMF is illustrated in Fig. 3, assuming light can be launched to all transverse modes.

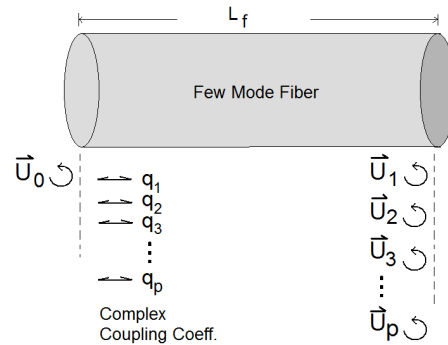


Fig. 3. Model for the interference in a few-mode fiber.

The field amplitudes of the modes depend on the complex coupling coefficient $q_l = |q_l|e^{j\varphi_l}$ for each mode l of the fiber. The reflected electric field of the l^{th} mode is modeled by $\bar{U}_l = |q_l|^2 \bar{U}_0 e^{-2j(\beta_l L_f + \varphi_l)}$ and the interference pattern generated by the reflections at the facets of the FMF are described by Eq. (5)

$$\begin{aligned}
I_{Real}(\lambda) &= \left| \overline{U}_0 + \dots + \overline{U}_p \right|^2 \\
&= \left| \overline{U}_0 \right|^2 \left(\underbrace{\left(1 + \sum_{l=1}^p |q_l|^4 \right)}_{DC \text{ Term}} + \underbrace{\left(\sum_{l=1}^p 2|q_l|^2 \cos(2(\beta_l L_f + \varphi_l)) \right)}_{High \text{ frequency (Absolute measurement)}} \right) \\
&\quad + \underbrace{\left(\sum_{l=1}^{p-1} \sum_{m=l+1}^p 2|q_l|^2 |q_m|^2 \cos(2((\beta_l - \beta_m)L_f + (\varphi_l - \varphi_m))) \right)}_{Low \text{ Frequency (Differential measurement)}} \right) \quad (5)
\end{aligned}$$

The DC term results from the sum of the amplitudes of the coupling coefficients of each mode. The high frequency terms contain information on the individual propagation constants for which *absolute* measurements can be obtained. The low frequency terms contain information about the relative differences between the propagation constants of the modes, from which *differential* measurements between modes can be obtained. This paper focuses on the virtual referencing of the high frequency terms in Eqs. (5) and (1a) since this allows for the measurement of *absolute* group delay and second order dispersion, avoiding the ambiguity possible with differential (relative) measurements. It is worth mentioning, however, that we are not precluded from making differential measurements using VRI. For the FMF experiment, the virtual referencing process is performed exactly as described in the previous section and the details are omitted for brevity.

3. Experimental method

Polarization modes in a Panda fiber and transverse modes in a four-mode FMF are characterized using VRI. In both measurements a tunable laser source (Agilent 81642A), with a built-in wavemeter (wavelength resolution of 0.1 pm), is swept from 1510 nm to 1640 nm. A wavelength accuracy of ± 15 picometers is ensured by the built in automatic wavelength calibration function of the wavemeter. Both experiments use a fiber optic circulator connected to a tunable laser and detector, as illustrated in Figs. 4(a) and 4(b). The tunable laser is connected to port 1 of the circulator and a detector (Thorlabs PDA10CS) is connected to port 3. Port 2 is connected to the device under test via different optical elements depending on the experiment. Each experiment measures the first and second order dispersion curves generated from a single scan of the tunable laser using VRI. The setup used for the characterization of the polarization modes of a Panda PM fiber is illustrated in Fig. 4(a). A polarization controller is used to ensure even power distribution into both polarization modes which effectively sets $\Delta = 0$ in Eq. (1). This allows both modes to be characterized simultaneously with high signal-to-noise ratio. Note that even if A_1 and A_2 are quite different (i.e. without the polarization controller), both modes can still be characterized simultaneously (though power will not be evenly distributed between modes). Although it is possible to measure each mode separately, simultaneous measurement of both modes is desirable since it increases accuracy by eliminating the possibility of thermal fluctuations in fiber length between scans. In order to characterize the transverse modes in an FMF using VRI and BSI longitudinal offset coupling is employed as illustrated in Figs. 4(b) and 4(c). This is achieved by using a translation stage to vary the gap distance between the FC/APC connector of the launch fiber and the FC/PC connector on the test fiber. This setup allows for variability in the power coupled to each of the higher order modes. The results of VRI measurements are then compared to those made using BSI.

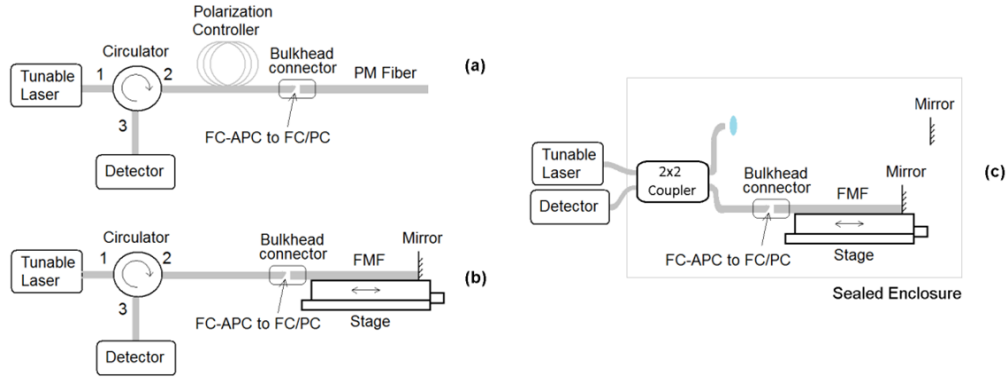


Fig. 4. Experimental setup for measurement of (a) polarization modes in PM fiber using VRI, (b) transverse modes in an FMF using VRI, and (c) Transverse modes using BSI.

4. Results

The results of the measurement of the group delay (first order dispersion) and the dispersion \times length (second-order dispersion extracted from the group delay data) of the modes in a Panda PM fiber are illustrated in Figs. 5(a) and 5(b) respectively. The results agree well with simulated curves for both polarization modes, provided by the manufacturer, Corning[®] Inc.

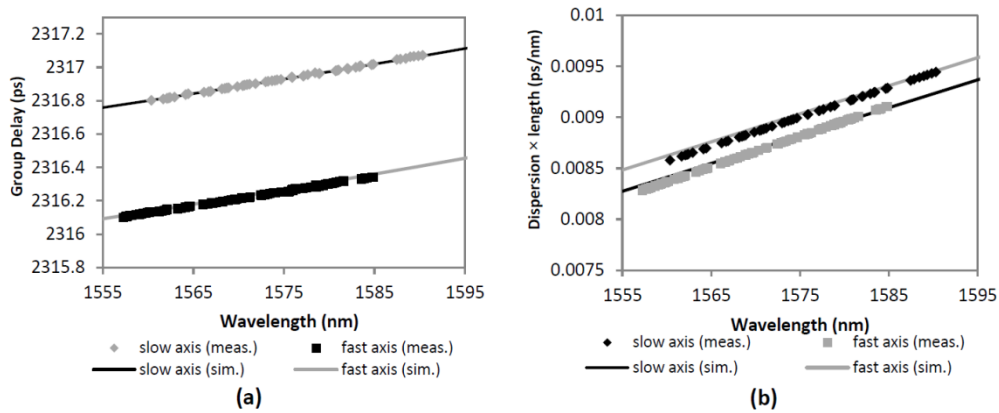


Fig. 5. Simultaneous absolute (a) group delay and (b) dispersion \times length measurements for both polarization modes of a 47.2 cm long Panda fiber

VRI based group delay and dispersion \times length measurements on a four mode FMF are compared to results obtained using conventional BSI in Figs. 6 and Figs. 7(a)-7(d) respectively. The low power coupled to each mode in the FMF increased the scatter in the group delay curves. As a result, the second order dispersion (dispersion \times length) had to be extracted directly from the balanced interferogram, which is possible using both BSI and VRI, as described in [22, 24, 25]. In the VRI experiment the first three modes of the fiber (LP01, LP11 and LP02) were characterized in one scan. The gap position was then adjusted and a second scan was performed to increase the coupled power into the LP21 mode. As a result, the VRI curves in Figs. 6 and Figs. 7(a)-7(d) were generated using only two scans, whereas, in the BSI experiment every point required a separate scan. It is important to note that the variation in the scatter observed between experiments is due to the differences in power coupling (variation in SNR) between experiments for a given mode. The results for both first and second order dispersion, however, agree well in both experiments.

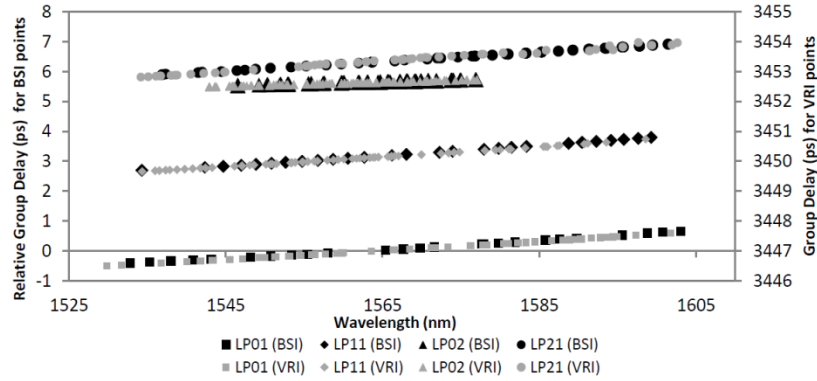


Fig. 6. Absolute group delay measurements of a 69.9 cm long few-mode fiber measured using Balanced Spectral Interferometry and Virtual Reference Interferometry

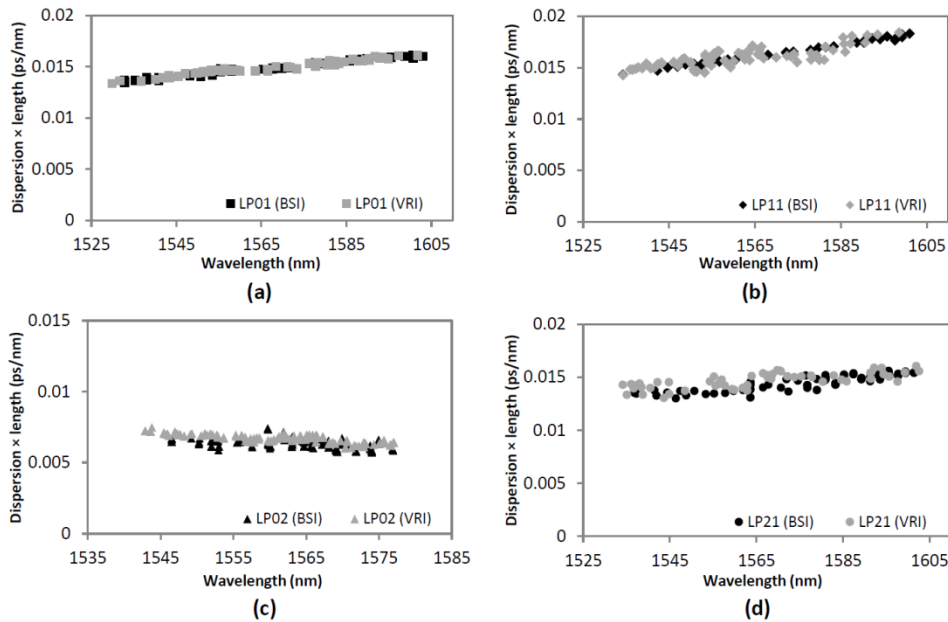


Fig. 7. Comparison of the dispersion \times length measurements for the (a) LP01 mode, (b) LP11, (c) LP02 mode, and (d) LP21 mode of a 69.9 cm length of few-mode fiber measured via Balanced Spectral Interferometry and Virtual Reference Interferometry.

5. Conclusion

We have demonstrated the measurement of first- and second-order dispersion of polarization modes in a Panda PM fiber and transverse modes in an FMF using VRI. The all-fiber experimental setup is simple, convenient and fast and allows sufficiently separated and excited fiber modes to be characterized simultaneously in a single scan.

Acknowledgments

The authors would like to thank Corning® Inc. for providing simulated curves for the Panda PM fiber. Michael Galle would like to thank the Vanier Canada Graduate Scholarship program for supporting this research. This project is funded by NSERC Discovery, CFI, and ORF Grants.